

# *Chapter 1*

## **Introduction**

Grain boundary migration is an important process during recrystallization and grain growth. The rate of migration determines the kinetics of these phenomena, and therefore is responsible for the evolution of microstructures, which have been proved to be closely related to many material properties. Nevertheless, little is known about the atomistic mechanisms in terms of grain boundary migration. Owing to the complicated geometry of a grain boundary with five degrees of freedom, the existing experimental techniques, e.g. transmission electron microscopy, to date are still unable to trace the atomic movements during grain boundary migration, especially at relatively high temperatures. These techniques therefore cannot effectively reveal the underlying mechanisms. Although there is no direct evidence, grain boundary migration has been implied to be related to types of diffusion processes (grain boundary diffusion and bulk diffusion) based on the fact that the migration and diffusion processes frequently possess nearly the same magnitude of activation enthalpy. In order to accurately determine atomic motions, the simulation technique molecular dynamics, which possesses profound advantages of high spatial and temporal resolutions, has been utilized. Some mechanisms have been observed. But these mechanisms seem to contradict each other, or they can only be applied to certain cases. The common feature of these mechanisms

obtained from simulations however indicates that grain boundary motion is not relevant to any diffusion process.

Besides the mechanisms of motion, grain boundary mobility is of great concern for industrial process optimization and modelling. This quantity can be accurately determined in well-designed bicrystalline experiments. However the difficulty of preparing bicrystals for various materials significantly limits the types of grain boundaries for study, such that it is hard to systematically measure the grain boundary mobility. In the past 15 years, the mobility for pure metals has also been evaluated and predicted through molecular dynamics simulations. The computed mobilities however are always found to be much larger than the maximum experimental data obtained in ultra-high-purity metals by one or more orders of magnitude. This drastic divergence is usually attributed to the absence of impurities in simulations, which are inevitably present in real materials. The impurities are expected to segregate in grain boundaries and therefore retard grain boundary motion significantly.

In this work, we exploit molecular dynamics to simulate grain boundary motion. We focus on  $\langle 111 \rangle$  tilt grain boundaries in pure Al, since the motion of these grain boundaries plays an important role in microstructural evolution during recrystallization and grain growth for conventional metals, and also because there are existing experimental data obtained in bicrystals for direct comparisons. The migration of the selected grain boundaries has been simulated in a wide temperature range with various magnitudes of driving force.

The contents of this work are organized as follows. In Chapter 2, the basics of grain boundary structure and its migration process are introduced on a general level. Together, the existing mechanisms regarding grain boundary migration and the mobility simulations performed previously by other groups are reviewed, respectively. Chapter 3 presents the simulation techniques relevant to this work. The techniques are mainly composed of molecular dynamics and the implementation of driving force for inducing grain boundary motion. In Chapter 4, the simulation results are provided. Based on these results as well as corresponding discussion, mechanism maps are proposed for boundary migration in polycrystals. In Chapter 5, we further concentrate on the boundary motion at a high temperature to compute mobilities, which are directly compared with experimental results. Finally, Chapter 6 gives a summary.



## *Chapter 2*

### **Fundamentals**

#### **2.1 Grain boundary structure**

A grain boundary (GB) is an internal interface which separates two grains of the same crystallography. On a macro level, there are in total eight geometric parameters required to comprehensively characterize a GB. As shown in Fig. 2.1, between the two adjacent grains, three parameters define a rotation angle  $\theta$  of the crystal lattice (called misorientation in the context) about a common axis; the two parameters of the normalized boundary normal  $\bar{n}$  describe the spatial orientation of the boundary plane; the last three parameters comprising a translation vector  $\bar{t}$  denote the relative shift between identical lattice points in the two grains of the same material. In reality, when investigating the relation between a GB and its properties, the translation vector is usually neglected, possibly because the vector is hard to be measured experimentally and also its effect on dynamic processes might be trivial. However some simulations [1] to calculate the global minimum of grain boundary energy indeed indicate that the translation vector plays an important role. By altering the vector and then relaxing boundary structure sufficiently, it is found that there are a large number of local minima of GB energy together with substantial energetic barriers among them. The differences among the minima can be large [1]. For example, the energy difference is as large

as about 30% for a  $\theta = 86.63^\circ$   $\langle 110 \rangle$  tilt GB in a general face-centered cubic (FCC) metal. The specific number of the energy minima is found to be a function of GB type as well as temperature. The question whether the translation vector also has an effect on a dynamic process, e.g. GB migration, is unclear. To avoid much complexity, the vector is not taken into consideration in this work. Only the misorientation and the spatial orientation of boundary plane are focused on.

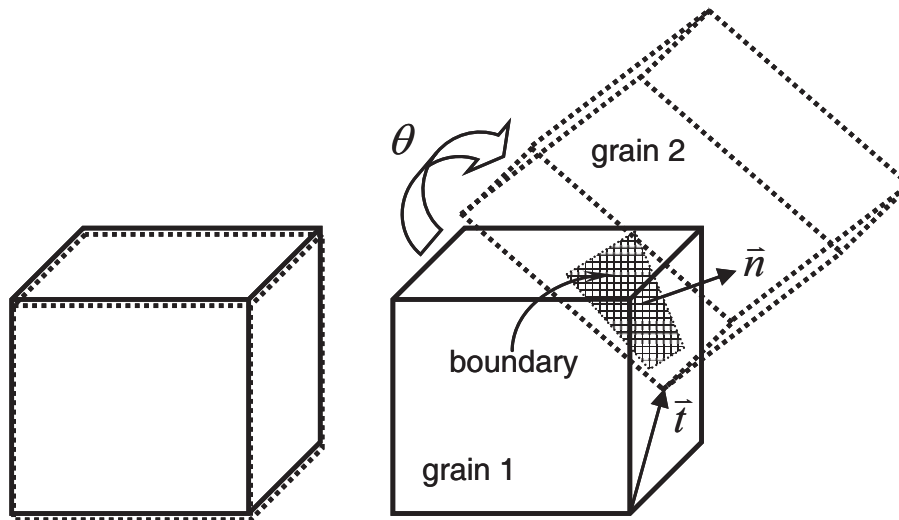


Fig. 2.1. Parameters for a geometrical description of a grain boundary.

Between the rotation axis and the boundary plane, there are distinct relations which give rise to different types of GBs. In the cases that the axis is perpendicular to the plane, twist GBs are obtained (Fig. 2.2a). When the axis is parallel to the plane, we have tilt GBs, which are further classified into symmetric or asymmetric ones, depending on whether the boundary normal has an identical or different description in the two adjoining grains, respectively (Fig. 2.2b). In comparison with the unique symmetric tilt GB for a given pair of a rotation axis and angle, an infinite number of asymmetric ones can occur.

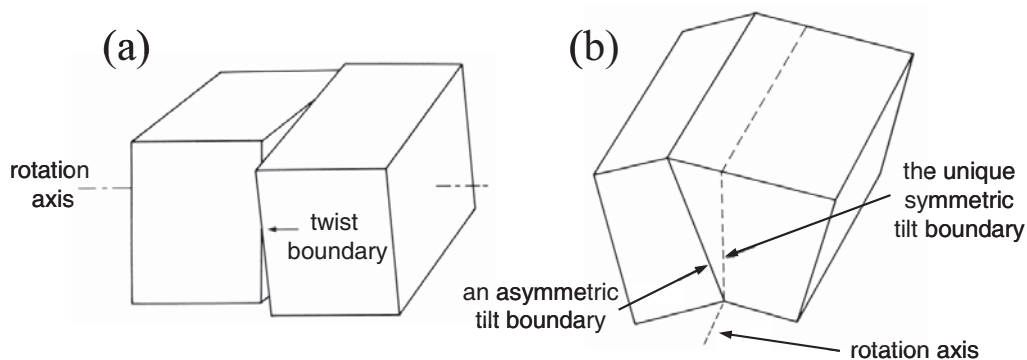


Fig. 2.2. Orientation of grain boundaries and rotation axes for different types of grain boundaries. (a) A twist boundary; (b) a symmetric and an asymmetric tilt boundary. (after[2])

From a microscopic view, GBs are composed of atoms in arrangements different from the one for a perfect crystal. The arrangement of boundary atoms reveals profound dissimilarity for GBs of small and large misorientations, i.e. so-called low-angle and high-angle GBs with a threshold  $\theta$  of about  $15^\circ$ . Low-angle GBs are formed by dislocation arrays together with nearly-perfect crystal regions. For a symmetric low-angle tilt GB, as drawn schematically in Fig. 2.3, a set of edge dislocations regularly distribute along the boundary plane with a spacing  $d$ , which can be calculated by  $d = b/\theta$  ( $b$  denotes the magnitude of Burgers vector associated with the edge dislocation), to create the misorientation. For an asymmetric tilt and a twist low-angle GBs, at least two sets of edge and screw dislocations, respectively, are needed. Since all these dislocations reside in GBs, they are named grain boundary dislocations (GBDs).

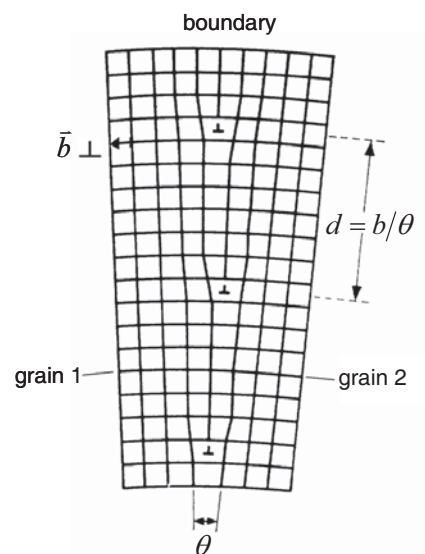


Fig. 2.3. Schematic of a low-angle tilt grain boundary formed by regularly distributed edge dislocations in nearly-perfect crystal regions. (after [2])

As indicated in Fig. 2.3, an increase in misorientation decreases the dislocation spacing, causing dislocation cores to come close to each other. When the misorientation becomes larger than about  $15^\circ$ , dislocation cores overlap substantially such that singular dislocations cannot be identified any more. The corresponding GBs are referred to as high-angle GBs. Although the structure of high-angle GBs might be thought of as a layer of disordered atoms, there are special misorientations which may provide GBs of relatively low energy. These misorientations refer to the cases when a coincidence site lattice (CSL) is generated. The 3-dimensional CSL represents an artificial lattice whose atomic positions are shared by the two adjacent crystals with the assumption that both crystal lattices are infinitely extended (Fig. 2.4). Since the two crystal lattices are periodic, the CSL must be periodic as well. Associated

with CSL, a quantity  $\Sigma$ , defined as the density ratio of ideal lattice sites to coincidence sites, then is commonly utilized to represent the corresponding misorientation and in turn the GB type. It should be noted that the CSL model merely concerns misorientation, but not a boundary plane. In practice, curved GBs frequently existing in polycrystals prevent unambiguous characterization of a specific boundary plane, thus misorientation is the unique measurable quantity. Using  $\Sigma$  to describe GBs of special misorientation becomes plausible. By contrast, for flat tilt GBs, misorientation together with a specific boundary plane need to be determined to comprehensively understand or describe a structure-property relation.

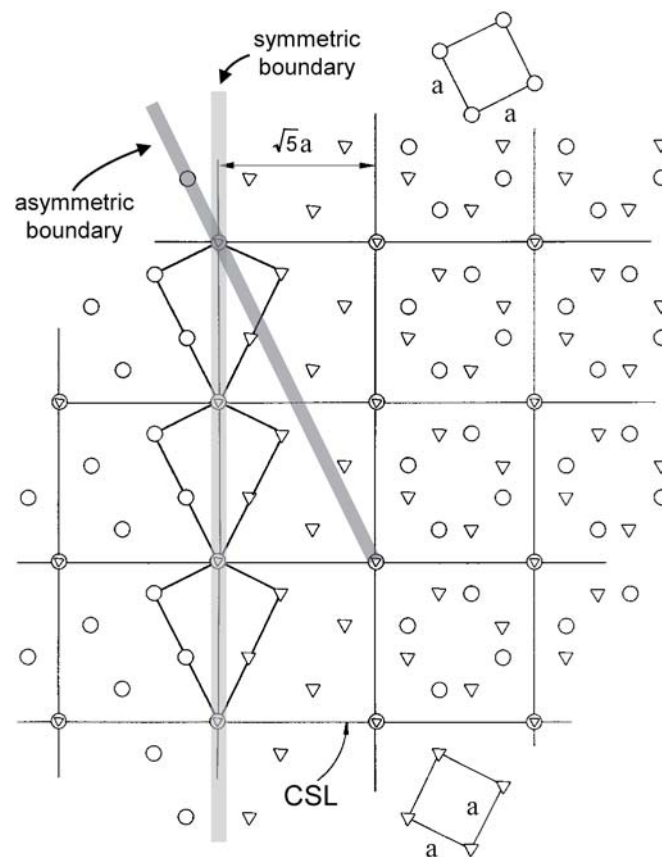


Fig. 2.4. Coincidence site lattice (CSL) and the structures of a twist GB (parallel to the paper plane shown on the right side), a symmetric tilt and an asymmetric tilt GB (both perpendicular to the paper plane given on the left side) in a cubic crystal lattice. All three GBs possess the same misorientation of  $36.87^\circ$  around the  $\langle 100 \rangle$  axis in a cubic crystal. These GBs are also of the same  $\Sigma$  equal to 5. The circles and triangles represent atoms in two grains, respectively. The lattice constant is denoted by  $a$ . (after [2])

As implied in the CSL construction, the  $\Sigma$  misorientations are discrete. When there is a deviation from these misorientations, it is proposed that a network of grain boundary dislocations is generated in GBs. These dislocations are of Burgers vectors of the displacement shift complete (DSC) lattice, which is the coarsest grid that comprises all lattice points of both crystal lattices (Fig. 2.5). Since the magnitudes of the Burgers vectors

associated with these GB dislocations are smaller than the ones for lattice dislocations, these dislocations are called secondary GB dislocations (SGBDs). The introduction of SGBD into  $\Sigma$  misorientation nevertheless still cannot compensate the deviation thoroughly, since the DSC lattice is discrete as well. For continuously changing misorientation, there must be cases for which other types of defects, e.g. local lattice distortion, take place.

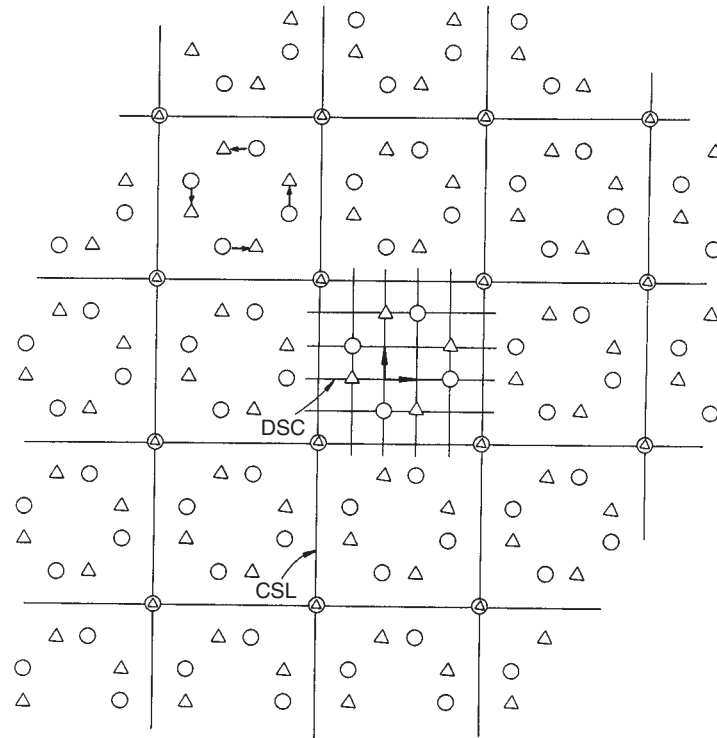


Fig. 2.5. Coincidence site lattice (CSL) and displacement shift complete (DSC) lattice for a  $36.87^\circ$   $\langle 100 \rangle$  twist grain boundary in cubic crystals. (after [2])

It should be noted that the question how special the  $\Sigma$  GBs are is subtle. Considering the relation between properties and misorientation, only very few GBs with low  $\Sigma$  values may reveal low boundary energy, while the others exhibit uniform high energy almost identical to the magnitude associated with GBs of general misorientations (Fig. 2.6). A correlation between kinetic parameters (GB migration mobility and its activation parameters) and the  $\Sigma$  misorientations is found in some studies, but not in others. In this sense, Wolf et al. [3] suggested that high-angle GBs should be classified into two types: special and general GBs. The former only concerns the  $\Sigma$  GBs giving rise to energy cusps (Fig. 2.6). All the other GBs pertain to general GBs. This suggestion is adopted in this work.

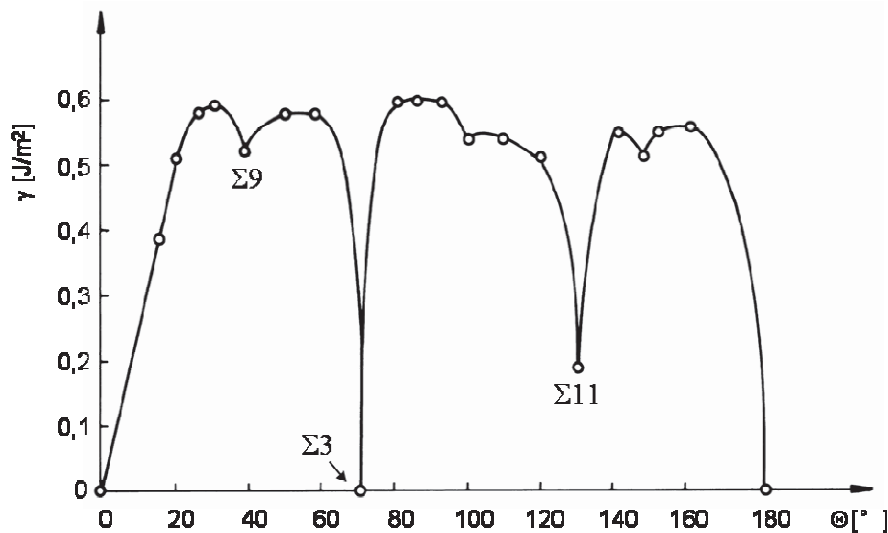


Fig. 2.6. Misorientation dependence of grain boundary energy for symmetric  $\langle 110 \rangle$  tilt boundaries in Al. The energy cusps are associated with several low- $\Sigma$  GBs. (after [4])

Up to now, the consideration of high-angle GB structure is confined to purely geometrical descriptions. According to Fig. 2.4, one may notice that there are large spaces present in the symmetric tilt GB. This structure is expected to be of high energy and thus being unstable. To lower the boundary energy, a structural relaxation takes place. The relaxation process usually doesn't change the periodicity of the CSL. But short-range shifts of atomic positions cause GBs to exhibit some structural disorder. Based on the analyses in terms of GB atoms through the radial distribution function, the structure of a high-angle GB at low temperatures is demonstrated to be solid-like, resembling glass [3, 5], as shown in Fig. 2.7a. The degree of the disorder is limited, as GBs still can be described by some kite-shaped structural units (Fig. 2.8). With increasing temperature, the disorder becomes further enhanced. For a temperature higher than a critical point, a high-angle GB undergoes a reversible structural transformation to be liquid-like in analogy to a bulk melt [3, 5], as illustrated in Fig. 2.7b. This transformation process is also referred to as GB premelting [6-9].



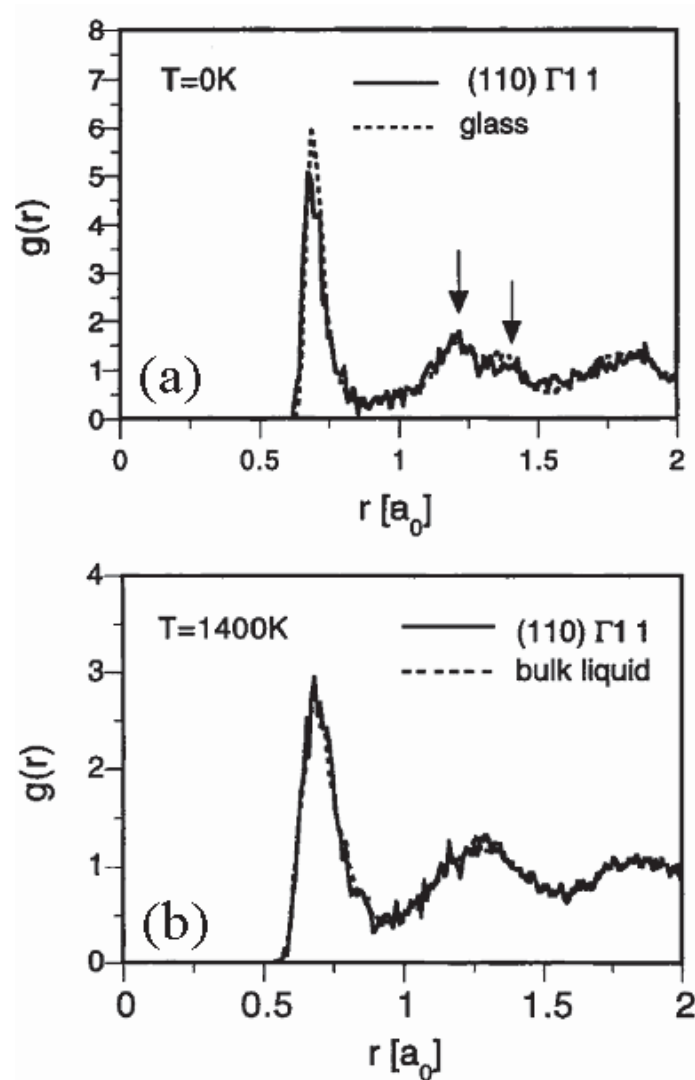


Fig. 2.7. Comparison of atomic distribution between (a) atoms in a  $\Sigma 11$  ( $\theta = 50.48^\circ$ )  $\langle 110 \rangle$  twist grain boundary at 0 K and atoms in glass; (b) atoms in the same boundary but at 1400 K and atoms in a bulk liquid. The distribution is quantified by the radial distribution function  $g(r)$ . The arrows in (a) indicate the split second peak. (after [5])

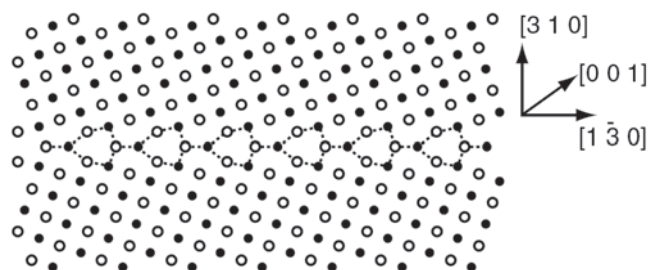


Fig. 2.8. Atomic structure of a  $36.87^\circ$  symmetric  $\langle 100 \rangle$  tilt grain boundary in Cu at 0 K. The filled and open circles represent atoms locating in alternating (200) planes. The kite-shaped structural units are outlined. (after [10])